applied sciences

MDPI

Article

Lumateperone Interact with S-Protein of *Ebola* Virus and TIM-1 of Human Cell Membrane: Insights from Computational Studies

Muhammad Muzammal [1], Ahmad Firoz [2,3], Hani Mohammed Ali [2,3], Arshad Farid [1], Muzammil Ahmad Khan [1,4] and Khalid Rehman Hakeem [2,3,5,*]

[1] Gomal Center of Biochemistry and Biotechnology, Gomal University, Dera Ismail Khan 29050, Pakistan
[2] Department of Biological Sciences, Faculty of Science, King Abdulaziz University, Jeddah 21589, Saudi Arabia
[3] Princess Dr Najla Bint Saud Al-Saud Center for Excellence Research in Biotechnology, King Abdulaziz University, Jeddah 21589, Saudi Arabia
[4] Department of Human Genetics, Precision Medicine Program, Sidra Medicine, Doha 26999, Qatar
[5] Department of Public Health, Daffodil International University, Dhaka 1207, Bangladesh
* Correspondence: kur.hakeem@gmail.com

Simple Summary: The present computational study shows that Lumateperone possesses a strong attraction to the S-Protein and TIM-1 receptor of the host as well as to their complex. It was observed that the binding energy of the S-Protein/TIM-1 complex decreases in the presence of Lumateperone. In conclusion, this computational study predicts the possibility of using Lumateperone against the *Ebola* virus as a therapeutic strategy.

Abstract: The *Ebola* virus outbreak in Africa is an unparalleled risk to society and to human health. Interventions that utilize the host cell receptor TIM-1 and the viral spike protein (S-protein) can be considered effective and suitable treatments. Initially, we identified Lumateperone as a candidate drug for the S-protein using the LEA3D tool; then using molecular modeling and docking, we investigated the binding efficiency of Lumateperone with the S-protein and its TIM-1 receptor. The present computational study shows that Lumateperone possesses a strong attraction to the S-protein and the TIM-1 receptor of the host as well as to their complex. It was observed that the binding energy of the S-protein/TIM-1 complex decreases in the presence of Lumateperone. A significant decrease of 395.75 kJ/mol (Lumateperone bound to the S-protein) and 517.19 kJ/mol (Lumateperone bound to the TIM-1 receptor) of binding energy was observed in the S-protein/TIM-1 complex in the presence of Lumateperone compared to their direct binding. We also noticed that Lumateperone was binding with the residues in the S-protein (Asn461) and the TIM-1 (Trp274 and Asn275) receptor that were involved in making the S-protein/TIM-1 complex. In the presence of Lumateperone, the simulation analysis also supports the above findings on the effectiveness of Lumateperone in delaying the establishment of the complex of the S-protein/TIM-1. In conclusion, this computational study predicts the possibility of Lumateperone as a therapeutic strategy against the *Ebola* virus.

Keywords: Lumateperone; S-protein/TIM-1 complex; *Ebola* virus; binding energy

Citation: Muzammal, M.; Firoz, A.; Ali, H.M.; Farid, A.; Khan, M.A.; Hakeem, K.R. Lumateperone Interact with S-Protein of *Ebola* Virus and TIM-1 of Human Cell Membrane: Insights from Computational Studies. *Appl. Sci.* **2022**, *12*, 8820. https://doi.org/10.3390/app12178820

Academic Editor: Cezary Czaplewski

Received: 8 June 2022
Accepted: 8 July 2022
Published: 2 September 2022

1. Introduction

The Filoviridae family, including the *Ebola* virus, causes haemorrhagic fevers and a high death rate in humans. Presently, there is no effective treatment for the *Ebola* virus [1]. The *Ebola* virus (EBOV) RNA genome is approximately 18.9 kb in size. It is a single-stranded, non-segmented (-)RNA and codes for at least eight different proteins. The nucleoprotein (NP), polymerase protein (L), VP24, VP30, and VP35 form the ribonucleoprotein complex. On the virion envelope, the glycoprotein (GP) forms spikes on the surface, while VP40 is associated with the inner surface, which is the matrix protein [1,2].

The *GP* gene encodes the surface glycoprotein (GP). It has vital roles in the pathogenesis and infection of the virus, and during virus replication, its expression is tightly controlled [3]. It has been documented recently that the level of GP1 and GP2 expression controls the production and release of the virus [4]. The *Ebola* virus comprises different structural proteins such as spike (S), envelope (E), membrane (M), and the nucleocapsid (N) proteins [4]. The S-protein is glycoprotein in nature. In human cells, the *Ebola* virus enters through the binding of the surface spike protein with a receptor protein (T-cell immunoglobulin mucin domain-1 (TIM-1)) present on the membrane of human cells. This facilitates the virus–host cell membrane fusion and receptor binding. A schematic representation of the inhibition of the virus S-protein through Lumateperone is shown in Figure 1.

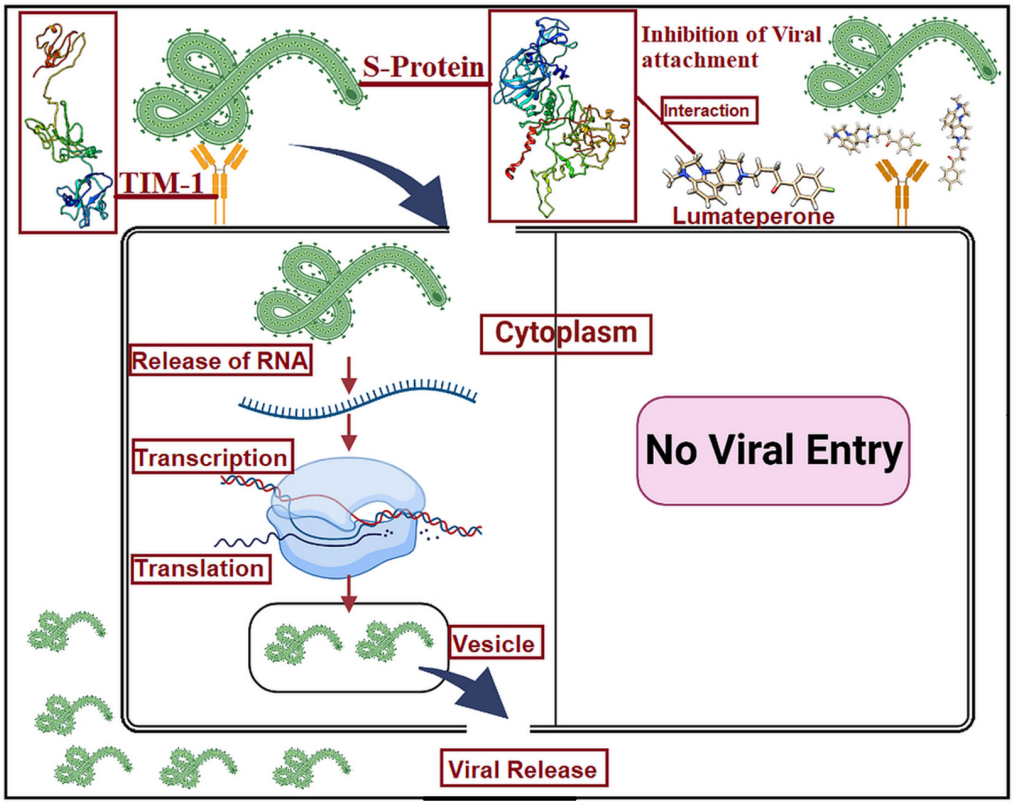

Figure 1. Graphical representation of the binding of the viral S-protein with the TIM-1 cellular receptor. The presence of Lumateperone inhibits the S-protein and TIM-1 interaction and eventually prevents viral entry into the cell.

In the endosomal compartment of human cells, several cell surface receptors facilitate filovirus attachment and incorporation, i.e., phosphatidylserine (PS) receptors [5,6] and C-type lectin receptors [7,8]. PS receptors do not bind with the virus glycoprotein (GP) but interact with PS on the surface of the virion lipid membrane, which causes the incorporation of virus particles into the endosomal compartment [6,9]. This process of viral entry is known as apoptotic mimicry [10,11].

The T-cell immunoglobulin mucin domain (TIM) family is one of the most important families of PS receptors [12]. The type I cell surface glycoproteins (GPs) are members of the TIM protein family. Whereas in mice the functional family members are four, "TIM-1, TIM-2, TIM-3, and TIM-4", in humans there are only three: "TIM-1, TIM-3, and TIM-4". Murine TIM-1 (mTIM-1) and mTIM-4 and human TIM-1 (hTIM-1) and hTIM-4 can assist as enveloped viral receptors, while the other members cannot [11,12].

Previously, Lumateperone has been reported as a serotonin transport inhibitor. It causes inhibition in a mesolimbic-specific manner, raising the glutamatergic N-methyl-D-aspartate (NMDA) GluN2B receptors phosphorylation in the human body [13]. There is no

information about the binding of Lumateperone with the S-protein of the *Ebola* virus and its host cells cognate receptor TIM-1.

Through this backdrop, the current study examines the binding of Lumateperone with the virus S-protein and the host cells cognate receptor TIM-1 using computational methods. The computational methods (molecular docking and simulation) are the best approaches to study this type of binding mechanism before experimental studies, which are costly and take more time.

In addition, the enhancement in the reliability, speed, and accuracy of computational docking approaches in last few years make it an appropriate alternative to drug design, which is structure-based. The current study includes molecular modeling and docking results of Lumateperone with the S-protein of the *Ebola* virus along with the host cell TIM-1, which is a virus S-protein cognate receptor in the human body.

2. Materials and Methods

2.1. Protein 3D Structure Prediction

The 3D structure of the *Ebola* virus S-protein and the human cell immunoglobulin mucin domain-1 (TIM-1 receptor) was designed using online tools I-TASSER. I-TASSER (Iterative Threading Assembly Refinement) is a bioinformatics method for predicting the three-dimensional structural model of protein molecules from amino acid sequences using a technique called fold recognition (or threading) [14]. The 3D models were verified using the PROCHECK tool in the form of a Ramachandran plot [15]. Ramachandran is used for the measurement of angles in amino acids (proteins). The protein sequence of the S-protein (Uniprot id# Q05320) and the TIM-1 receptor (Uniprot id# Q96D42) was obtained from the online Uniprot database [16].

2.2. Ligand Selection

Ligand selection was performed using the LEA3D tool [17] with its virtual screening tool. LEA3D is used to perform computer-aided drug design based on molecular fragments.

2.3. Drug Target Prediction

Drug target prediction was carried out using the Swiss Target predication tool [18]. The Swiss Target predication tool predicts results in the form of a pie chart identifying the actual mode of action of the drug in the body.

2.4. Molecular Dynamic Simulation

Molecular Dynamic Simulation was performed using the iMods online tool [19]. This is an online tool and is useful for exploring the collective motions of biological macromolecules. As we had identified Lumateperone as a candidate target for the S-protein, we further confirmed the interaction between the TIM-1 receptor and the Lumateperone molecule. With the iMods online tool, we calculated B-factor/mobility, eigenvalues, the covariance map, and the elastic network of the docked complex of the TIM-1 receptor and the Lumateperone molecule [19].

2.5. Protein–Protein Docking

ClusPro2.0 [20] (an automated rigid body-docking tool) was used in the presence and absence of Lumateperone for the S-protein/TIM-1 protein docking analysis. With respect to the clustering properties and by considering various protein parameters, this tool helps in screening docked conformations. The filtered conformations selection was based on the assessment of empirical free energy. For the assessment of free energy, both the lower desolvation and electrostatic energy were also considered. Piper is a rigid docking tool based on FFT, which provides 1000 low-energy outcomes; therefore, it helps the ClusPro clustering program detect native sites. Among the predicted models, only the lowest binding energy model was selected.

2.6. Molecular Docking Analysis of S-Protein, TIM-1 with Lumateperone

AutoDock Tools 1.5.6 [21] (molecular docking program) were used for the estimation of binding free energy of the S-protein and TIM-1 with Lumateperone. From the PubChem database [22], the canonical SMILES id of Lumateperone was obtained. CHIMERA 1.11.2 [23] was used to visualize the 3D structures. The affinity of the S-protein and TIM-1 to bind with Lumateperone was examined by AutoDock Vina 1.1.2 [21]. Discovery Studio 2020 [24] and Ligplus+ tool [25] visualized and analyzed the results of the docking studies.

2.7. Physiochemical Properties of Lumateperone

The physiochemical properties of Lumateperone were obtained using the online SwissADME tool. The SwissADME tool [26] provides lipophilicity, water solubility, pharmacokinetics, medical chemistry, and druglike properties of Lumateperone.

3. Results

3.1. Structural Modeling

The 3D models of the S-protein and TIM-1 were designed using the I-TASSER tool and then cross-checked through the RaptorX (http://raptorx.uchicago.edu) tools as in Figure 2. The 3D models were further verified by Ramachandran plot. The Ramachandran plot verified that in both the S-protein and the TIM-1 structure, residues were present in the favored and allowed regions. In the case of the TIM-1 structure, residues of favored and allowed regions were 56.1% and 35.7%, respectively, (Supplementary Figures S1–S3) while in the case of the S-protein, residues present in favored and allowed regions were 47.1% and 36.9%, respectively, (Supplementary Figures S1 and S2).

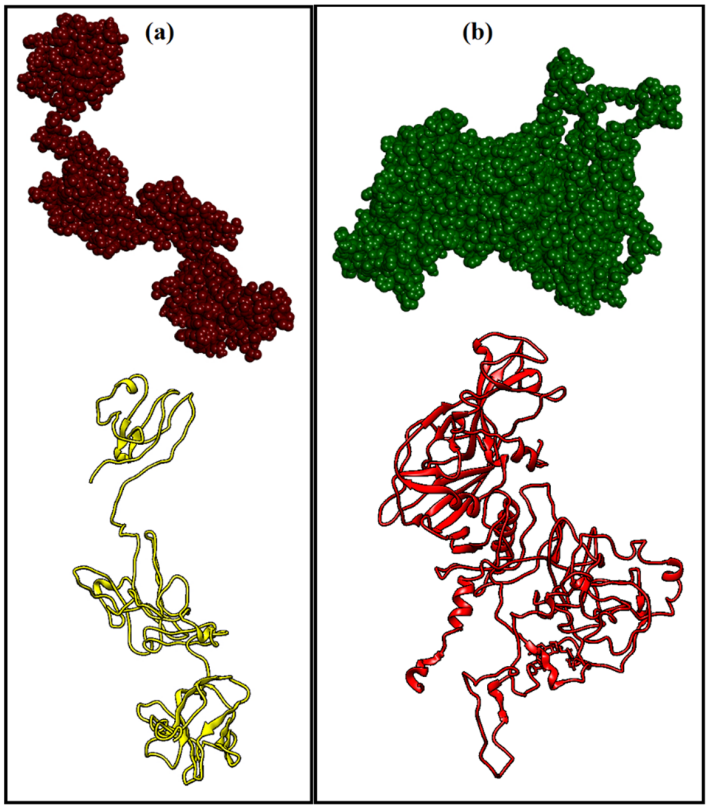

Figure 2. (**a**) 3D structure of the TIM-1 receptor protein, both ribbon and balloon; (**b**) 3D structure of the *Ebola* virus S-protein, both ribbon and balloon, designed using the I-TASSER tool.

3.2. Ligand Selection and Its Validation

Considering a best possible drug for the *Ebola* virus S-protein using its 3D models, LEA3D predicted Lumateperone as the best possible candidate drug for the S-protein by

screening the United States Food and Drug Administration (FDA or USFDA) reported drugs. After the identification of Lumateperone as a candidate drug, further computational study was undertaken. The mode of action of Lumateperone in the human body is shown in Supplementary Figure S3. However, the physicochemical properties of Lumateperone are summarized in Table 1.

Table 1. Physiochemical properties of Lumateperone.

Physiochemical Properties		**Lipophilicity**	
Formula	$C_{24}H_{28}FN_3O$	Log *P* o/w (LOGP value)	3.68
Molecular weight	393.5 g/mol	Log *P* o/w (XLOGP3 value)	3.77
Number of heavy metal	29	Log *P* o/w (WLOGP value)	3.19
Number of aromatic heavy metal	12	Log *P* o/w (MLOGP value)	3.43
Fraction Csp3	0.46	Log *P* o/w (SILICOS-IT value)	3.71
Number of rotatable bonds	5	Consensus Log *P* o/w	3.56
Number H bond accepters	3	Pharmacokinetics	
Number H bond donors	0	CYP2C19 inhibitor (Cytochrome P450 2C19 inhibitor)	No
Molar refractivity	124.38	CYP2C9 inhibitor (Cytochrome P450 2C9 inhibitor)	No
TPSA (topological polar surface area)	26.79 A^2	CYP2D6 inhibitor (Cytochrome P450 2D6 inhibitor)	Yes
Consensus Log *P* o/w	3.56	CYP3A4 inhibitor (Cytochrome P450 3A4 inhibitor)	Yes
Water Solubility		Log K_p (skin permeation)	−6.02 cm/s
Log S (ESOL)	−4.63	CYP1A2 inhibitor (Cytochrome P450 1A2 inhibitor)	No
Solubility	9.20×10^{-3} mg/mL; 2.34×10^{-5} mol/L	P-glycoprotein substrate	Yes
Class	Moderately soluble	Blood–Brain barrier permeant	Yes
Log S (Ali)	−4.03	Gastrointestinal absorption	High
Solubility	3.71×10^{-2} mg/mL; 9.42×10^{-5} mol/L		
Class	Moderately soluble		
Log S (SILICOS-IT)	−6.15		
Solubility	2.78×10^{-4} mg/mL; 7.06×10^{-7} mol/L		
Class	Poorly soluble		

3.3. Molecular Docking

3.3.1. Protein–Protein Docking

In the case of protein–protein docking, we first performed docking of the S-protein and the TIM-1 receptor. Residues involved in interactions in both the S-protein and the TIM-1 receptor are summarized in Table 2, while the 2D schematic representation of interactions is shown in Figure 3a. The lowest docking energy among all the predicted models of the S-protein and the TIM-1 receptor complex was about 900 kJ/mol in the absence of Lumateperone. A 3D representation of the viral protein and the TIM-1 receptor with respective energy is shown in Figure 4.

Table 2. The interacting residues and bonding in protein–protein and protein–substrate interaction.

Receptor–Ligand Interaction	Type of Interaction	Interacting Residues
S-protein–Lumateperone	Pi-Donar Hydrogen Bond	**Asn461**
	Pi Sigma	Ala349
	Alkyl	Ile626,Val353
	Pi-Alkyl	Ala459
TIM-1 receptor–Lumateperone	Van der Waals	Thr241, Ile246, Asn277, Ser201, Asn276, Asp271
	Conventional Hydrogen Bond	Asn221
	Carbon Hydrogen Bond	**Asn275**
	Pi–Cation	Arg219
	Pi–Pi stacked	**Trp274**
	Pi–Alkyl Bond	Ala245
Protein–Protein Interaction (S-Protein/TIM-1)	**Type of Interaction**	**Interacting Residues**
S-protein residues TIM-1 receptor residues	Hydrogen Bond Interaction	Lys56, Arg54, Asn461, Asn514, Asn463, Glu359, Ser363, Thr367, Val181, Asp632, Lys633, Thr363, Asp364, Gln278, Asn275, Trp274, Lys317, Ser303, Ala339, Lys338, Gln336

Note = Bold residues are residues of S-protein and TIM-1 protein that interact with Lumateperone.

It was observed that in presence of Lumateperone, the binding energy of the S-protein/TIM-1 decreases during protein–protein interaction. A significant decrease of 395.75 kJ/mol (Lumateperone initially binds to the S-protein) and 517.19 kJ/mol (Lumateperone initially binds to the TIM-1 receptor) of binding energy was detected in the presence of Lumateperone during the binding of the S-protein/TIM-1 compared with their (S-protein/TIM-1) direct binding (in the absence of Lumateperone) as shown in Figure 5. The site of the interaction of the S-protein and the TIM-1 receptors before and after the docking of Lumateperone, i.e., the interaction of the S-protein and the TIM-1 receptor when Lumateperone initially docked with the TIM-1 protein and vice versa, is shown in Table 3. Thus, it can be assumed that the binding of the S-protein and the TIM-1 receptor can be hindered by Lumateperone and vice versa. Furthermore, we can conjecture that Lumateperone would definitely make it easier to repurpose/design effective treatment to prevent the virus from entering cells.

3.3.2. Protein–Substrate/Drug Docking

In case of protein–substrate/drug docking, first we performed the docking of the S-protein with Lumateperone. S-protein residues involved in interacting with Lumateperone include Asn461, Ala349, Ile626, Val353, and Ala459 through different bonding as shown in Table 2 and Figure 3b. Among these residues, Asn461 was the common residue of the S-protein that was involved in interacting with Lumateperone as shown in Figure 3. Moreover, in the case of Lumateperone and TIM-1 docking, residues involved in interacting included Thr241, Ile246, Asn277, Ser201, Asn276, Asp271, Asn221, Asn275, Arg219, Trp274, and Ala245 through different bonding shown in Table 2. Additionally, common TIM-1 residues that were involved in interacting with both S-protein and Lumateperone include Trp274 and Asn275. A complete description of results is shown in Figure 3.

3.4. Molecular Dynamic Simulation of TIM-1 and Lumateperone Docked Complex

Figure 6a shows the main chain deformability of the TIM-1 and Lumateperone docked complex deformed at each of its residues. The location of the chain 'hinges' can be derived from the high deformability regions. The B-factor of the majority of the interacting residues was between 250–300 (Figure 6a). The iMOds finding confirms our docking results in Figure 3.

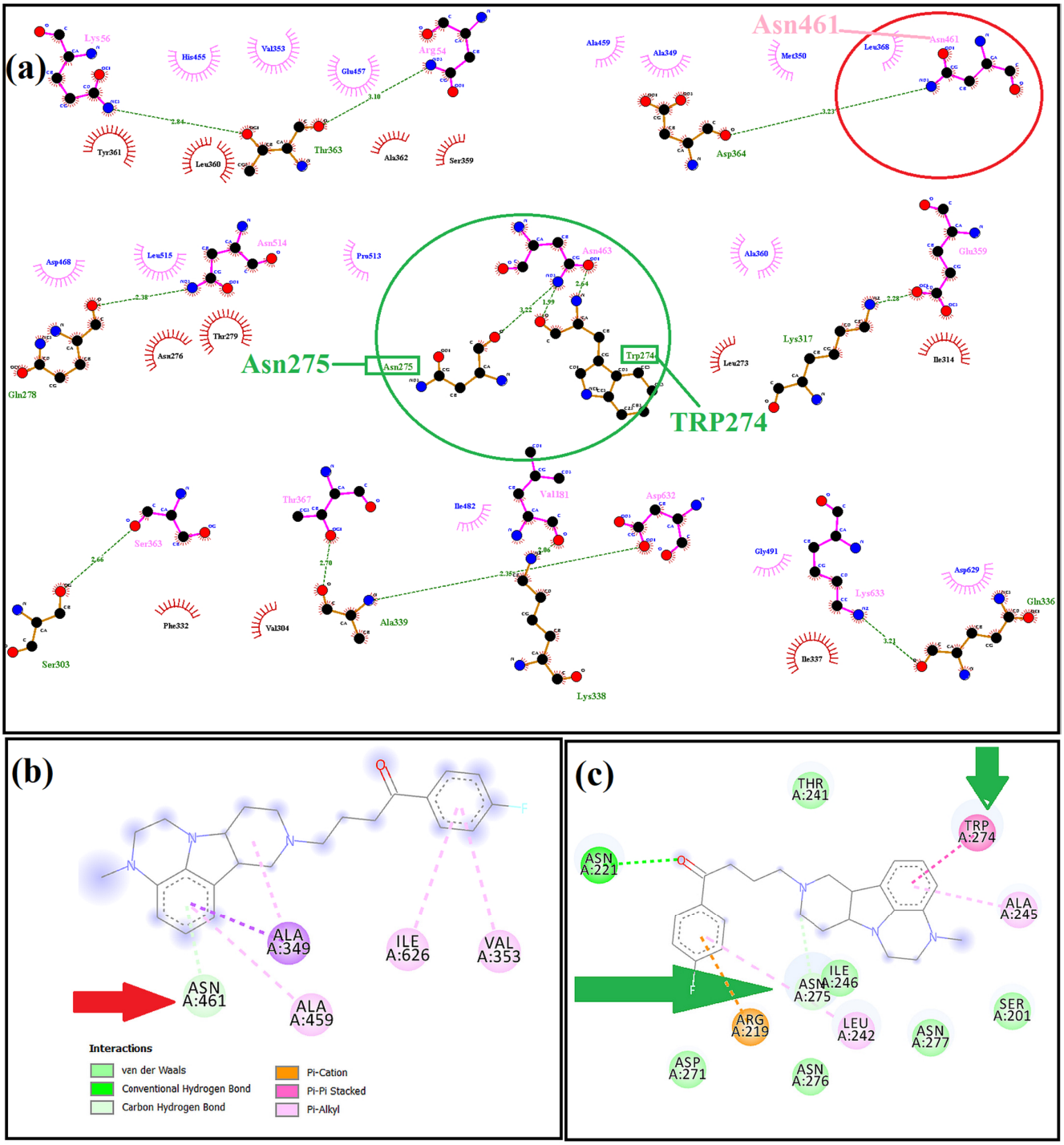

Figure 3. (**a**) 2D representation of the S-protein/TIM-1 interaction showing the interacting residues of both proteins; the green circle shows the residues of the TIM-1 protein that were interacting with Lumateperone; the red circle shows the residues of the S-protein that were involved in interacting with Lumateperone; (**b**) 2D representation of Lumateperone and S-protein docking, while the red arrow shows the common interacting residue of the S-protein; (**c**) 2D representation of Lumateperone and TIM-1 docking; the green arrow shows the common interacting residues on the TIM-1 protein.

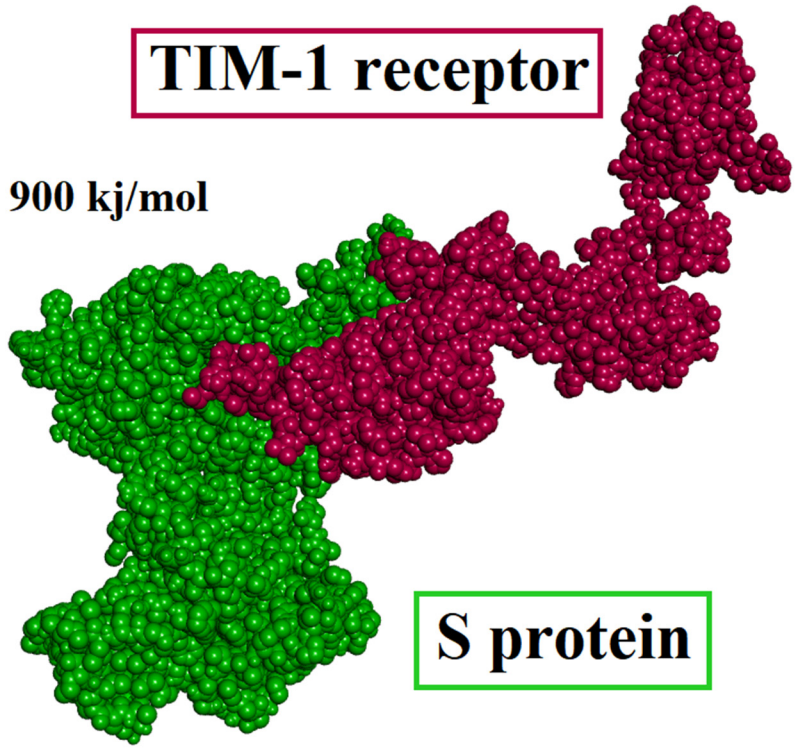

Figure 4. S-protein/TIM-1 protein docked complex showing the 900 kJ/mol as the binding energy of the system in the absence of a Lumateperone molecule.

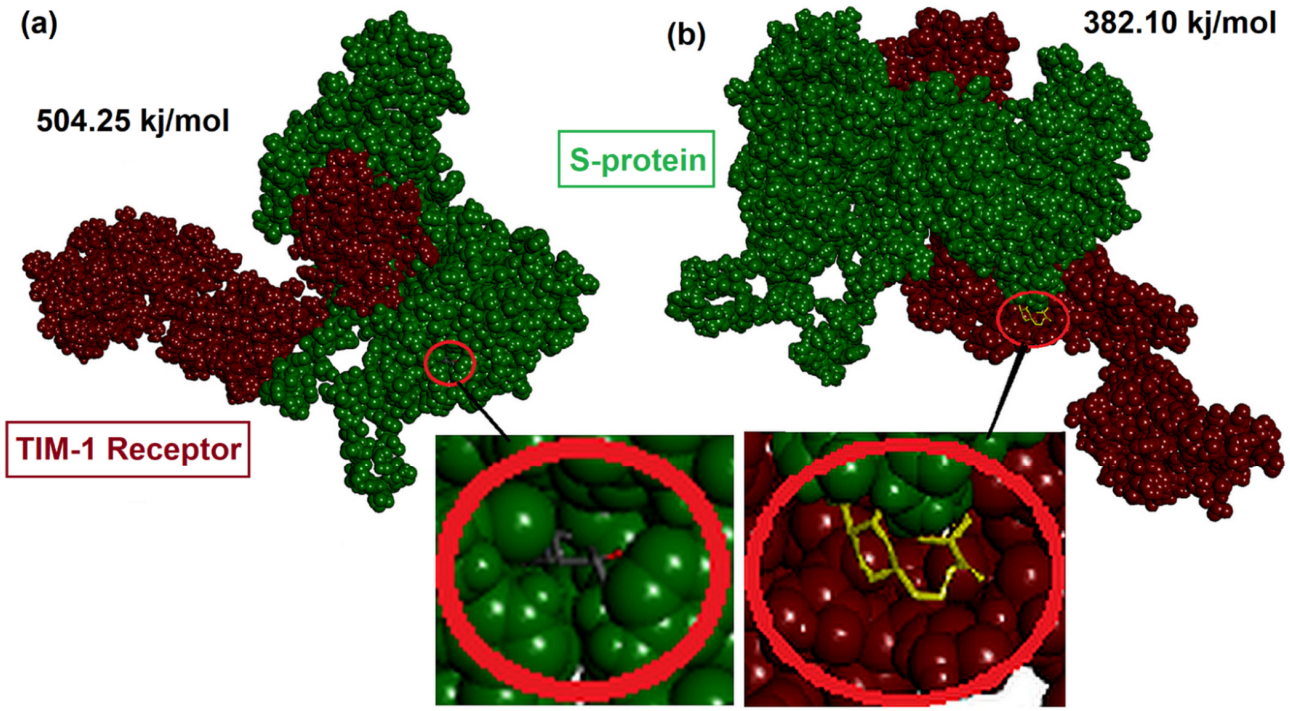

Figure 5. (**a**) S-protein/TIM-1 protein docking complex showing the binding energy of the system in the presence of Lumateperone (Lumateperone is docked with the S-protein); (**b**) S-protein/TIM-1 protein docking complex showing the binding energy of the system in the presence of Lumateperone (Lumateperone is docked with the TIM-1 protein).

Table 3. Site of interaction of the S-protein and the TIM-1 receptors before and after docking of Lumateperone.

	S-protein docking sites	TIM-1 receptor docking sites	Type and number of Bonds
Lumateperone is docked to the S-protein	Lys633, Leu481, Asp629, Asp632, Thr367, Glu472, Asn514	Lys338, Gln336, Lys318, Ala339 His285, Gln278	5 hydrogen 2 unfavorable bond
Lumateperone is docked to the TIM-1 protein	Gln567, Asp419	Met 1, Thr155	2 hydrogen bonds

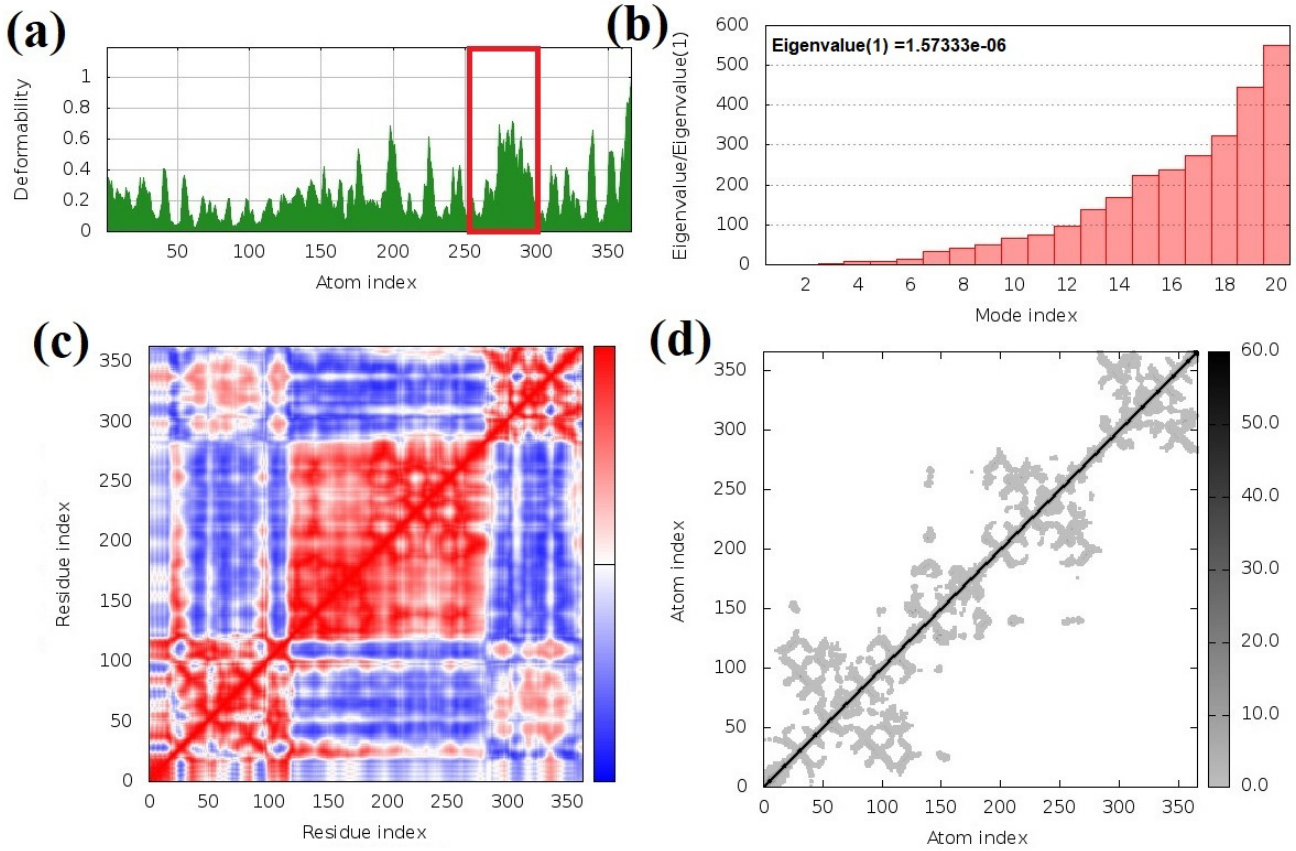

Figure 6. Simulation results of the TIM-1/Lumateperone complex: (**a**) B-factor mobility of binding residues; most of the B-factor residues are present between position 250–300 highlighted in the red box; (**b**) TIM-1/Lumateperone complex shows the low eigenvalues; at eigenvalue f, the complex was found to be 1.57330×10^{-6} and confirmed to be an unstable structure; (**c**) covariance map showing the stability of binding residues in the red portion; (**d**) elastic network showing the least stiff TIM-1/Lumateperone complex, as the least grey color shows that this complex can be broken with small energy.

Figure 6b shows the motion stiffness of the complex by normal mode linked with the eigenvalue. The motion stiffness value has a direct relation to the energy needed to distort the structure. Deformation is easier with a low eigenvalue. The eigenvalue of our complex was about 1.573330×10^{-6}. This means that less energy will be required to deform the structure (as in Figure 6b).

Figure 6c shows the covariance matrix, which indicates a connection among pairs of residues, i.e., whether they experience correlated (red), uncorrelated (white), or anti-correlated (blue) motions. From Figure 6c, you can see that most of the residues in the TIM-1 protein and Lumateperone correlated with each other, giving the best coupling matrix.

Figure 6d reports the pairs of atoms that are linked by springs described by the elastic network model. Each dot in the graph represents one spring between the corresponding pair of atoms. The dots are colored according to the stiffness; the stiffer springs are

indicated by darker grays and vice versa. From the figure, you can see that our elastic network is less stiff, which shows the best dock complex of the TIM-1 and the candidate drug Lumateperone molecule (Figure 6d). Overall, finding iMOds confirms our docking results in Figure 3 about the position of the interacting residues and the interaction of the drug with the TIM-1 and the S-protein.

4. Discussion

More than 27,000 infections and 11,000 deaths have been reported due to the *Ebola* virus (EBOV) outbreak in West Africa [27]. The primary method of treatment is still sympathetic care, although numerous *Ebola* virus candidate vaccines and treatment strategies have been evaluated [28]. However, *Ebola* virus candidate vaccines have serious side effects such as increased levels of inflammation and lymphopenia, in spite of a modest efficacy [28].

In humans and other primates, the *Ebola* and Marburg viruses cause haemorrhagic fever. There is no cure or effective treatment and 50% to 90% of cases are fatal [27].

Identifying and understanding the way the virus enters cells can help with treatment. New bioinformatics-based techniques, developed by John Chiorini at NIDCR, are used by researchers for the identification of the TIM-1 protein as a receptor for *Ebola* and Marburg viruses. For infecting cells, both the *Ebola* and Marburg viruses use the TIM-1 as a receptor as proven by successive experiments [29]. Their study also proved that on epithelial cells (that line several tissues in the body such as mucosal surfaces of the airways and in the eyes), the TIM-1 protein is widely expressed. Moreover, Andrew in 2011, also reported that infection in cells expressing the TIM-1 protein by infectious Zaire *Ebola* virus were blocked by the ARD5 antibody. The results suggest that being able to block *Ebola*'s entry into epithelial cells, perhaps with a human-compatible version of the ARD5 antibody, might provide a way to prevent initial infection and potentially limit the spread of the disease during an outbreak [29].

Keeping these points in mind, we tried to propose a new candidate drug to control the entry of *Ebola* virus into the cell. We identified the candidate drug using the LEA3D tool, which predicted Lumateperone as a possible candidate drug to inhibit *Ebola* virus entry into the cell.

The physiochemical, water solubility, lipophilicity, and pharmacokinetics properties of Lumateperone were also calculated. Lumateperone's chemical formula is $C_{24}H_{28}FN_3O$, and its molecular weight is estimated to be 393.5 g/mol. It has a total of 29 heavy metal atoms. Lumateperone acts as a CYP2D6 inhibitor (Cytochrome P450 2D6 inhibitor) in the body. Complete descriptions of its properties are summarized in Table 1.

Lumateperone is a butyrophenone, a typical neuroleptic for schizophrenia therapy, developed by Intra-Cellular Therapies, approved from Bristol-Myers Squibb. It has recently been approved for bipolar depression and other neural indications. Somnolence and dehydrated mouth are the most common side effects [13].

There are no previous data that may show the direct antiviral activity of Lumateperone, but Vela et al., 2020, while working on human viruses to screen the antiviral molecules from different compounds, documented that infection of B lymphocytes, caused by a human herpesvirus, Epstein–Barr virus (EBV), were inhibited by butyrophenone [30].

In another study, Diffley in 2021 screened and identified several drugs that might be repurposed to treat COVID-19. He reported that Trifluperidol, which is also butyrophenone and previously was used in the treatment of mania and schizophrenia, is effective to cleave the coronavirus enzyme Nsp14 mRNA G-N7 cap methyltransferase in the human body [31].

Sze'kelyhidi et al., 2005, documented that for the hepatitis B virus (HBV), the validated target is the SR protein-specific kinase-1 (SRPK-1). The authors designed and synthesized different tricyclic quinoxaline derivatives as antiviral agents having the potential to inhibit kinase and which were selective and active for SRPK-1 kinase. According to experimentally determined LogP and LogS values, many of these compounds possess drug-like characteristics. Among the identified compounds, one of the compounds was butyrophenone, which was effective in inhibiting the HBV virus from entering the cell [32].

In the current study, we initially performed protein–protein docking of the S-protein and the TIM-1 receptor, and docking sites were noted (Figure 3). We found that the S-protein interacted with the TIM-1 protein through 11 different residues (Table 2). However, among those 11 residues, Lys56, Arg54, and Val181 were the residues that were previously known to be significant for viral entry into the cell. These results confirm the finding of previous studies [33–37].

In the next step, Lumateperone was docked with the S-protein. The S-protein/Lumateperone docked complex interacted through five different residues (Table 2); between them, two residues, i.e., Ala459 and Asn461, were the residues of the highly glycosylated mucin-like domain of the S-protein (MCD). The MCD domain is from 313–464 on the S-protein [37]. Previously, it has been documented that a major function of the MCD domain is to protect the glycoproteins from cell surface proteolysis and also protect the cells from attack by other cells [38]. From these results, we can presume that binding Lumateperone to the residues of the MCD domain of the S-protein may affect the efficiency of viral entry and also lessen the viral protective core.

In the case of the TIM-1/Lumateperone docked complex, TIM-1 and Lumateperone interacted through 11 different residues as shown in Table 2. Between them, two residues, i.e., Asn461 and Trp274, were the common residues that were also involved in the interaction with the S-protein during the S-protein/TIM-1 docked complex formation (Figure 3). These results also indicate that Lumateperone could be a possible inhibitor of S-protein/TIM-1 docking.

Furthermore, we then docked Lumateperone with the S-protein and then docked that complex with the TIM-1 receptor. Similarly, in the next step, we docked Lumateperone first with the TIM-1 receptor, and then that complex was docked with the S-protein. In this way, we obtained two different complexes. In the first, Lumateperone was initially docked with the S-protein. In the second, Lumateperone was initially docked with the TIM-1 receptor as shown in Figure 5. We found that in both the complexes, Lumateperone decreased the binding energies of the S-protein/TIM-1 complex. Lumateperone was docked either with the S-protein or the TIM-1 receptor before complex formation (Figures 4 and 5). Moreover, we knew that the lower the binding energy, the more unstable the complex would be [39]. So, we obtained a more unstable complex in the case where Lumateperone was bound either to the S-protein or the TIM-1 receptor in the complex. Not only did the bind energies of the complexes decrease, but the interaction between the S-protein and the TIM-1 protein also decreased in terms of interacting residues, the position of the interacting residues, and the bonding of interacting residues as in Table 3.

From various evidence, the results attained in this study showed that Lumateperone binds mostly to the region of the S-protein which is vital in binding with host cell [40].

Moreover, it was observed that Lumateperone binds to the TIM-1 at sites which served as a medium for virus entrance, i.e., Lys56, Arg54, and Val181 [37,40]. Therefore, outcomes of the current computational study propose that the use of Lumateperone prevents virus infection. It is obvious from the computational study arrangement that blocking the attachment of the host cell receptors to the virus by this inhibition mechanism and the inhibition of the virus protein cellular entrance might be an effective therapeutic target. However, this needs to be experimentally validated prior to translational intervention.

Hence, in the host system, the availability of Lumateperone may facilitate various mechanisms at the same time and thus promote removal and/or neutralization of virus infection.

5. Conclusions

The *Ebola* pandemic provides a stark landscape for clinical outcomes, with exceedingly high mortality rates. There is an urgent need to find viable treatments to combat *Ebola* outbreaks. In this context, the findings of this computational study indicate that Lumateperone shows promising results as an effective antiviral drug. However, supporting these findings requires more experimental validation.

Supplementary Materials: The following supporting information can be downloaded at: https://www.mdpi.com/article/10.3390/app12178820/s1, Figure S1: 3D structure validation of TIM-1 protein through Ramachandran plot; Figure S2: 3D structure validation of TIM-1 protein through Ramachandran plot; Figure S3: Mode of action of Lumateperone in human body.

Author Contributions: Data curation, M.M., A.F. (Ahmad Firoz), M.A.K. and K.R.H.; Formal analysis, A.F. (Ahmad Firoz), H.M.A., A.F. (Arshad Farid) and K.R.H.; Funding acquisition, M.M. and H.M.A.; Investigation, A.F. (Ahmad Firoz) and A.F. (Arshad Farid); Methodology, M.M., A.F. (Ahmad Firoz), H.M.A., A.F. (Arshad Farid), M.A.K. and K.R.H.; Project administration, H.M.A., M.A.K. and K.R.H.; Resources, M.M., M.A.K. and K.R.H.; Visualization, M.M.; Writing—original draft, M.M., A.F. (Ahmad Firoz), H.M.A., A.F. (Arshad Farid), M.A.K. and K.R.H. All authors have read and agreed to the published version of the manuscript.

Funding: This Project was funded by the Deanship of Scientific Research (DSR), at King Abdulaziz University, Jeddah, under grant no. DF-553-130-1441. The author, therefore, acknowledge with thanks DSR for technical and financial support.

Institutional Review Board Statement: Not applicable.

Informed Consent Statement: Not applicable.

Data Availability Statement: The computational data is stored in the password protected personal computer of M.M., which is available upon request.

Acknowledgments: This Project was funded by the Deanship of Scientific Research (DSR), at King Abdulaziz University, Jeddah, under grant no. DF-553-130-1441. The author, therefore, acknowledge with thanks DSR for technical and financial support. We also thank the developers of all the freely available online tools i.e., PROCHECK, I-TASSER, LigPlus+ and ClusPro 2.0.

Conflicts of Interest: The authors declare no conflict of interest.

References

1. Geisbert, T.W.; Hensley, L.E. *Ebola* virus: New insights into disease aetiopathology and possible therapeutic interventions. *Expert Rev. Mol. Med.* **2004**, *6*, 1–24. [CrossRef] [PubMed]
2. Feldmann, H.; Klenk, H.-D. Marburg and *Ebola* viruses. *Adv. Virus Res.* **1996**, *47*, 1–52.
3. Feldmann, H.; Jones, S.; Klenk, H.-D.; Schnittler, H.-J. *Ebola* virus: From discovery to vaccine. *Nat. Rev. Immunol.* **2003**, *3*, 677–685. [CrossRef] [PubMed]
4. Mohan, G.S.; Ye, L.; Li, W.; Monteiro, A.; Lin, X.; Sapkota, B.; Pollack, B.P.; Compans, R.W.; Yang, C. Less is more: *Ebola* virus surface glycoprotein expression levels regulate virus production and infectivity. *J. Virol.* **2015**, *89*, 1205–1217. [CrossRef] [PubMed]
5. Brunton, B.; Rogers, K.; Phillips, E.K.; Brouillette, R.B.; Bouls, R.; Butler, N.S.; Maury, W. TIM-1 serves as a receptor for Ebola virus in vivo, enhancing viremia and pathogenesis. *PLoS Negl. Trop. Dis.* **2019**, *26*, 13. [CrossRef]
6. Jemielity, S.; Wang, J.J.; Chan, Y.K.; Ahmed, A.A.; Li, W.; Monahan, S.; Bu, X.; Farzan, M.; Freeman, G.J.; Umetsu, D.T. TIM-family proteins promote infection of multiple enveloped viruses through virion-associated phosphatidylserine. *PLoS Pathog.* **2013**, *9*, e1003232. [CrossRef]
7. Muzammal, M.; Khan, M.A.; Mohaini, M.A.; Alsalman, A.J.; Hawaj, M.A.A.; Farid, A. In Silico Analysis of Honeybee Venom Protein Interaction with Wild Type and Mutant (A82V + P375S) *Ebola* Virus Spike Protein. *Biologics* **2022**, *2*, 45–55. [CrossRef]
8. Powlesland, A.S.; Fisch, T.; Taylor, M.E.; Smith, D.F.; Tissot, B.; Dell, A.; Pohlmann, S.; Drickamer, K. A novel mechanism for LSECtin binding to *Ebola* virus surface glycoprotein through truncated glycans. *J. Biol. Chem.* **2008**, *283*, 593–602. [CrossRef]
9. Buzon, M.J.; Seiss, K.; Weiss, R.; Brass, A.L.; Rosenberg, E.S.; Pereyra, F.; Yu, X.G.; Lichterfeld, M. Inhibition of HIV-1 integration in ex vivo-infected CD4 T cells from elite controllers. *J. Virol.* **2011**, *85*, 9646–9650. [CrossRef]
10. Mercer, J.; Helenius, A. Vaccinia virus uses macropinocytosis and apoptotic mimicry to enter host cells. *Science* **2008**, *320*, 531–535. [CrossRef]
11. Miller, E.H.; Obernosterer, G.; Raaben, M.; Herbert, A.S.; Deffieu, M.S.; Krishnan, A.; Ndungo, E.; Sandesara, R.G.; Carette, J.E.; Kuehne, A.I. *Ebola* virus entry requires the host-programmed recognition of an intracellular receptor. *EMBO J.* **2012**, *31*, 1947–1960. [CrossRef] [PubMed]
12. Lee, H.-H.; Meyer, E.H.; Goya, S.; Pichavant, M.; Kim, H.Y.; Bu, X.; Umetsu, S.E.; Jones, J.C.; Savage, P.B.; Iwakura, Y. Apoptotic cells activate NKT cells through T Cell Ig-Like Mucin-Like–1 resulting in airway hyperreactivity. *J. Immunol.* **2010**, *185*, 5225–5235. [CrossRef] [PubMed]
13. Celanire, S.; Poli, S. (Eds.) *Small Molecule Therapeutics for Schizophrenia*; Springer: Cham, Switzerland, 2015.
14. Yang, J.; Yan, R.; Roy, A.; Xu, D.; Poisson, J.; Zhang, Y. The I-TASSER Suite: Protein structure and function prediction. *Nat. Methods* **2015**, *12*, 7–8. [CrossRef]

15. Laskowski, R.A.; MacArthur, M.W.; Moss, D.S.; Thornton, J.M. PROCHECK: A program to check the stereochemical quality of protein structures. *J. Appl. Crystallogr.* **1993**, *26*, 283–291. [CrossRef]
16. UniProt Consortium. UniProt: A hub for protein information. *Nucleic Acids Res.* **2015**, *43*, 204–212. [CrossRef] [PubMed]
17. Douguet, D. e-LEA3D: A computational-aided drug design web server. *Nucleic Acids Res.* **2010**, *38*, W615–W621. [CrossRef]
18. Antoine, D.; Olivier, M.; Vincent, Z. Swiss Target Prediction: Updated data and new features for efficient prediction of protein targets of small molecules. *Nucleic Acids Res.* **2019**, *47*, W357–W364.
19. López-Blanco, J.R.; Aliaga, J.I.; Quintana-Ortí, E.S.; Chacón, P. iMODS: Internal coordinates normal mode analysis server. *Nucleic Acids Res.* **2014**, *42*, W271–W276. [CrossRef]
20. Kozakov, D.; Hall, D.R.; Xia, B.; Porter, K.A.; Padhorny, D.; Yueh, C.; Vajda, S. The ClusPro web server for protein–protein docking. *Nat. Protoc.* **2017**, *12*, 255. [CrossRef]
21. Gaillard, T. Evaluation of AutoDock and AutoDock Vina on the CASF-2013 benchmark. *J. Chem. Inf. Model.* **2018**, *58*, 1697–1706. [CrossRef]
22. Available online: https://pubchem.ncbi.nlm.nih.gov/ (accessed on 10 January 2022).
23. Pettersen, E.F.; Goddard, T.D.; Huang, C.C.; Couch, G.S.; Greenblatt, D.M.; Meng, E.C.; Ferrin, T.E. UCSF Chimera—A visualization system for exploratory research and analysis. *J. Comput. Chem.* **2004**, *25*, 1605–1612. [CrossRef] [PubMed]
24. Dassault Systemes. *BIOVIA, Discovery Studio Modeling Environment, Release 2017*; Dassault Systèmes: San Diego, CA, USA, 2016.
25. Laskowski, R.A.; Swindells, M.B. LigPlot+: Multiple ligand–protein interaction diagrams for drug discovery. *J. Chem. Inf. Model.* **2011**, *51*, 2778–2786. [CrossRef] [PubMed]
26. Daina, A.; Michielin, O.; Zoete, V. SwissADME: A free web tool to evaluate pharmacokinetics, drug-likeness and medicinal chemistry friendliness of small molecules. *Sci. Rep.* **2017**, *7*, 42717. [CrossRef] [PubMed]
27. Ogawa, H.; Miyamoto, H.; Nakayama, E.; Yoshida, R.; Nakamura, I.; Sawa, H.; Takada, A. Seroepidemiological prevalence of multiple species of filoviruses in fruit bats (*Eidolon helvum*) migrating in Africa. *J. Infect. Dis.* **2015**, *212* (Suppl. 2), S101–S108. [CrossRef]
28. Maslow, J.N. The cost and challenge of vaccine development for emerging and emergent infectious diseases. *Lancet Glob. Health* **2018**, *6*, e1266–e1267. [CrossRef]
29. Kondratowicz, A.S.; Lennemann, N.J.; Sinn, P.L.; Davey, R.A.; Hunt, C.L.; Moller-Tank, S.; Meyerholz, D.K.; Rennert, P.; Mullins, R.F.; Brindley, M. T-cell immunoglobulin and mucin domain 1 (TIM-1) is a receptor for Zaire Ebolavirus and Lake Victoria Marburgvirus. *Proc. Natl. Acad. Sci. USA* **2011**, *108*, 8426–8431. [CrossRef]
30. Vela, J.M. Repurposing sigma-1 receptor ligands for COVID-19 therapy? *Front. Pharmacol.* **2020**, *11*, 1716. [CrossRef]
31. Diffley, J.F. Author's overview: Identifying SARS-CoV-2 antiviral compounds. *Biochem. J.* **2021**, *478*, 2533–2535. [CrossRef]
32. Székelyhidi, Z.; Pató, J.; Wáczek, F.; Bánhegyi, P.; Hegymegi-Barakonyi, B.; Ero, D.; László, O. Synthesis of selective SRPK-1 inhibitors: Novel tricyclic quinoxaline derivatives. *Bioorg. Med. Chem. Lett.* **2005**, *15*, 3241–3246. [CrossRef]
33. Mpanju, O.M.; Towner, J.S.; Dover, J.E.; Nichol, S.T.; Wilson, C.A. Identification of two amino acid residues on *Ebola* virus glycoprotein 1 critical for cell entry. *Virus Res.* **2006**, *121*, 205–214. [CrossRef]
34. Manicassamy, B.; Wang, J.; Jiang, H.; Rong, L. Comprehensive analysis of *Ebola* virus GP1 in viral entry. *J. Virol.* **2005**, *79*, 4793–4805. [CrossRef] [PubMed]
35. Lee, J.E.; Fusco, M.L.; Hessell, A.J.; Oswald, W.B.; Burton, D.R.; Saphire, E.O. Structure of the *Ebola* virus glycoprotein bound to an antibody from a human survivor. *Nature* **2008**, *454*, 177–182. [CrossRef] [PubMed]
36. Wang, J.; Manicassamy, B.; Caffrey, M.; Rong, L. Characterization of the receptor-binding domain of Ebola glycoprotein in viral entry. *Virol. Sin.* **2011**, *26*, 156–170. [CrossRef]
37. Jain, S.; Martynova, E.; Rizvanov, A.; Khaiboullina, S.; Baranwal, M. Structural and functional aspects of *Ebola* virus proteins. *Pathogens* **2021**, *10*, 1330. [CrossRef] [PubMed]
38. Carraway, K.L.; Hull, S.R. Cell surface mucin-type glycoproteins and mucin-like domains. *Glycobiology* **1991**, *1*, 131–138. [CrossRef]
39. Jena, A.B.; Kanungo, N.; Nayak, V.; Chainy, G.B.N.; Dandapat, J. Catechin and curcumin interact with S protein of SARS-CoV2 and ACE2 of human cell membrane: Insights from computational studies. *Sci. Rep.* **2021**, *11*, 2043. [CrossRef]
40. Modrof, J.; Mühlberger, E.; Klenk, H.D.; Becker, S. Phosphorylation of VP30 impairs *Ebola* virus transcription. *J. Biol. Chem.* **2002**, *277*, 33099–33104. [CrossRef]